INTERNATIONAL JOURNAL OF AUTOMOTIVE AND MECHANICAL ENGINEERING (IJAME)
ISSN: 2229-8649 e-ISSN: 2180-1606
VOL. 17, ISSUE 1, 7687 – 7694
DOI: https://doi.org/10.15282/ijame.17.1.2020.16.0571

ORIGINAL ARTICLE

Effect of Pulse Currents on Weld Geometry and Angular Distortion in Pulsed GTAW of 304 Stainless Steel Butt Joint

Agus Widyianto, Ario Sunar Baskoro* and Gandjar Kiswanto

Department of Mechanical Engineering, Faculty of Engineering, Universitas Indonesia, Depok 16424, Indonesia. Phone: +62-21-7270032; Fax: +62-21-7270033

ABSTRACT – In this research, the effect of pulse currents on the weld geometry and angular distortion in pulsed GTAW (PGTAW) process in 3 mm thick SS-304 autogenous butt weld joint was investigated. Welding method uses pulse current and continuous current. The mean current and welding speed were kept constant with the peak current and base current were varied. During pulsed GTAW process, the arc condition was captured directly using a charge-coupled device (CCD) camera. Weld geometry was carried out using a digital microscope. Distortion was measured using Coordinate Measuring Machine (CMM). The results show that the peak current and base current have an influence on weld geometry and angular distortion. The weld geometry on pulsed GTAW was produced wider of weld bead width than continuous GTAW. However, angular distortion on continuous GTAW was higher than pulsed GTAW. Pulsed GTAW can widen the weld bead by 0.57% - 25.09%, but can reduce distortion by 15.15%-88.17%. As compared with weld geometry to the continuous GTAW, the widest result occurs at peak current 212A and base current 40A. The smallest of distortion on pulsed GTAW was achieved at peak current 138A and base current 80A.

ARTICLE HISTORY
Revised: 7th Oct 2019
Accepted: 10th Dec 2019

KEYWORDS
Pulse GTAW; Weld geometry, Angular distortion; SS-304

INTRODUCTION

Welding is one of the technologies that are widely used in the manufacturing industry. Gas tungsten arc welding (GTAW) is one of the most widely used welding methods in industrial sectors. GTAW can be operated without employing filler metals; this method is known as autogenous welding [1]. After the welding process is complete, the quality of the weld can be seen visually from the weld geometry (weld bead and depth of penetration) then proven by other tests. Changes in the shape of the specimen can occur after the welding process, commonly called distortion. Distortion gives a bad effect on the specimen when it will be assembled.

Stainless steel sheets with thin and medium thickness are widely used in automobiles, aerospace components, pressure vessels, etc [2]. Stainless steel sheets are suitable for joining with the pulsed GTAW process. There are 2 pulse levels in the welding current: the pulse current (I_p) is the higher current and the base current (I_b) is the lower current of short or long time interval [3,4]. Figure 1 shows the pulsed GTAW process parameters. Pulsed GTAW has many advantages over continuous GTAW process, such as improve arc stability, decrease the total heat input to the workpiece, minimize the width of the HAZ and increase the depth/width ratio of weld bead [5]. Using the pulsed GTAW process can easily controlled weld penetration, weld pool and weld quality. In addition, the absorption of gas by the weld pool and the tendency of heat cracks can be reduced [6].

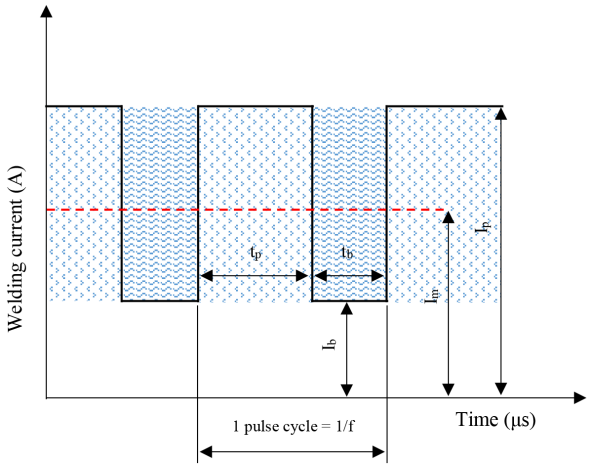

Figure 1. Pulsed GTAW process parameters [7].

*CORRESPONDING AUTHOR | Ario Sunar Baskoro | ✉ ario@eng.ui.ac.id

Heat input in the pulsed GTAW can be calculated from the mean current meanwhile heat input in the continuous GTAW can be calculated from the continuous current. Control of heat input can be made with adjustments peak current, base current and duty cycle [8]. The heat input in pulsed GTAW can be calculated by using Eq. (1) [6]:

$$HI = \frac{\eta V I_m}{S} \tag{1}$$

where, V, I_m, S and η are voltage, mean current, welding speed and arc efficiency (usually assumed to be 60% for pulsed GTAW) [7], respectively. The value of mean current (I_m) can be found out by using Eq. (2) [8].

$$I_m = \frac{I_p t_p + I_b t_b}{t_p + t_b} \tag{2}$$

where, I_p, I_b, t_p, and t_b are peak current, base/background current, time peak current and time base current, respectively. In the industries, stainless steel material in the form of thin sheets is one of the most frequently used materials. Pulsed GTAW process can produce good weld bead geometry using material stainless steel. The fusion welding will produce relatively higher heat inputs so there are many problems in thin sheets of stainless steel welds. The problems are the distortion of joint, porosity, melt through buckling and variation in penetration [9].

A lot of research on the conventional welding process to studies about weld bead geometry as GTAW [10, 11], GMAW [12] and SMAW [13]. Balasubramanian [14] reported about using Taguchi method to the optimisation of weld bead geometry on pulsed GTAW. Pal K [15] reviewed the effect of pulsed parameters on weld quality such as arc stability, weld geometry, HAZ width & distortion, microstructure, porosity content and mechanical properties. Hu Shengsun [16] reported that constant mean current PGTAW can reduce the hardness and make equiaxed grains by increasing pulse frequency of 21% Cr ferritic stainless steel. Distortion can be reduced by several techniques carried out before the process (clamping method [17]), during the process (dynamically controlled low stress no distortion method [18]) and after the welding process (laser shock processing method [19]).

Based on previous studies, distortion must occur in the welding process. Several methods have been explained to reduce distortion in the specimen. However, there were not many studies that discuss the pulse current method with the same mean current to reduce distortion. This study uses the pulse current method to reduce distortion and influence on weld geometry. Therefore, the objective of this study was to investigate the influence of pulse current GTAW parameters on weld bead geometry (top bead width and back bead width) and distortion (longitudinal bending distortion and angular distortion) of SS-304. The results were compared with continuous current GTAW.

EXPERIMENT METHODS

In this experiment, SS-304 was chosen witha thickness of 3 mm. The dimension of specimens in 50 × 120 mm and it was joined employing butt joints method. The welding experiment was carried out using a GeKaMac power TIG 2200 DC pulse welding machine with specifications 1 phase input voltage, 230 V, 50-60 Hz and current range 5-220 A. Single-pass of autogenous pulsed GTAW was made along the centerline of the butt joint specimen. The top and back weld zone was shielded by argon gas with a flow rate of 11 L/min and 3 L/min, respectively. The schematic of the experimental apparatus illustration is shown in Figure 2.

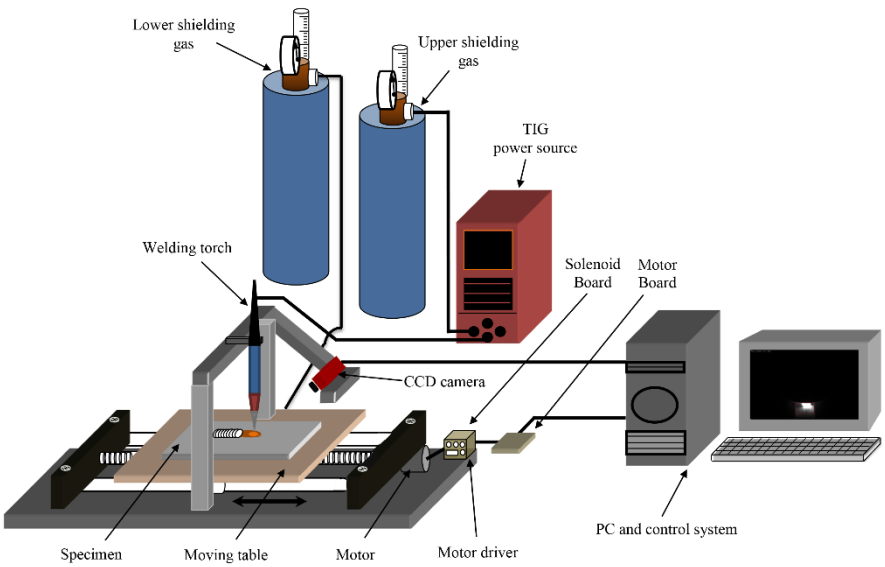

Figure 2. Schematic of pulsed GTAW apparatus.

Before welding, the surfaces of all specimens were cleaned by 80 until 400 grit flexible abrasive papers than clean residual impurities in the specimen with acetone solution. Chemical compositions of SS-304 used are given in Table 1. The welding parameters and the pulse conditions of the process that in this experiment are shown in Table 2 and Table 3, respectively.

Table 1. Chemical composition of the SS-304 (% by weight)

Element	C	Si	Mn	P	S	Ni	Cr
SS-304	< 0.07	< 0.75	< 2.00	< 0.045	< 0.030	8.00 - 10.50	17.50 - 19.50

Table 2. Welding conditions used in the experiment.

Parameter	Unit	Value
Power source	dimensionless	DCEN
Welding current	A	40 - 212
Welding speed	mm/sec	2.0
AWS classification	dimensionless	2% Th-W
Electrode diameter	mm	1.6
Nominal arc length	mm	2
Shielding gas	dimensionless	99,99% Argon
Upper shielding gas flow rate	L/min	11
Lower shielding gas flow rate	L/min	3

The voltage reading indicated by the welding machine was used to calculate heat input. For each pulse conditions, the mean current was kept the same at 100±0.5 A but the peak and base currents were varied. During the welding process, a Guppy Pro F-032B CCD camera was used for capturing the images of pulsed arc [20, 21]. The visualization test of top bead width and back bead width along the weld line was measured by using the Dino-Lite with measurement distance of 10 cm with 9 points for all of the welded specimens (see in Figure 3(a)).

The distortion measurement was calculated with the mean vertical displacement method. The distortion test was measurement using a Mitutoyo Coordinate Measuring Machine (CMM) M443. There were 12 points measurement, 4 points in the top, 4 points in the middle and 4 points in the bottom of the specimens. The distance of each point from the edge of 5 mm. Figure 3(b) shows the schematic illustration of measurement distortion. The result of measurement was used to calculate the longitudinal bending distortion and angular distortion. The longitudinal bending distortion U (mm) can be calculated from this mean vertical displacement in Eq. (3) [22]. Figure 3(c) shows that A, B, C and D were the mean vertical displacement values of each point. The angular distortion δ (rad) was estimated from the measured vertical displacement using Eq. (4) [23].

$$\mathrm{U} = \frac{(\mathrm{A}+\mathrm{B})-(\mathrm{C}+\mathrm{D})}{2} \tag{3}$$

$$\delta(\mathrm{rad}) = \frac{U_R + U_L - 2U_c}{55(60\text{-}5)} \tag{4}$$

RESULTS AND DISCUSSION

Pulse Arc Profile

The pulse arc profiles were shown in Figure 4. There were 2 current conditions, peak current and base current on parameters 35-A until 35-C for example. The parameter 35-A with a peak current of 138A and the base current of 80A has an arc profile of 6.1 mm and 4.2 mm, respectively. Whereas the arc profile formed on the 35-C parameter is 7.2 mm and 2.3 mm with peak current and the base current of 212A and 40A, respectively. So that increasing of peak current can widen the arc profile while decreasing of base current can shrinkage the arc profile. In addition, the arc profile can determine the width of the weld bead that will be formed. If the arc profile was wide, the weld bead would be wide, but if the arc profile was narrow, the weld bead would be narrow. So directly arc profile can affect the weld bead geometry (width of weld bead) was received by the specimens [24].

Table 3. Pulsed GTAW and Continuous GTAW process parameters.

No	Code	Peak current (A)	Base current (A)	Peak time (ms)	Base time (ms)	Frequency (Hz)	Duty cycle (%)	Mean current (A)	Welding speed (mm/s)	Arc efficiency (%)	Mean voltage (V)	Heat input (kJ/mm)
1	35-A	138	80	70	130	5	35	100.3	2.0	60	12.50	376.13
2	35-B	175	60	70	130	5	35	100.25	2.0	60	12.50	375.94
3	35-C	212	40	70	130	5	35	100.2	2.0	60	12.50	375.75
4	50-A	120	80	100	100	5	50	100	2.0	60	12.25	367.50
5	50-B	140	60	100	100	5	50	100	2.0	60	12.25	367.50
6	50-C	160	40	100	100	5	50	100	2.0	60	12.00	360.00
7	65-A	111	80	130	70	5	65	100.15	2.0	60	12.00	360.54
8	65-B	122	60	130	70	5	65	100.3	2.0	60	12.00	361.08
9	65-C	133	40	130	70	5	65	100.45	2.0	60	11.75	354.09

No	Code	Current (A)	Welding Speed (mm/s)	Arc Efficiency (%)	Voltage (V)	Heat Input (kJ/mm)
10	100-A	100	2.0	60	12.00	360.00

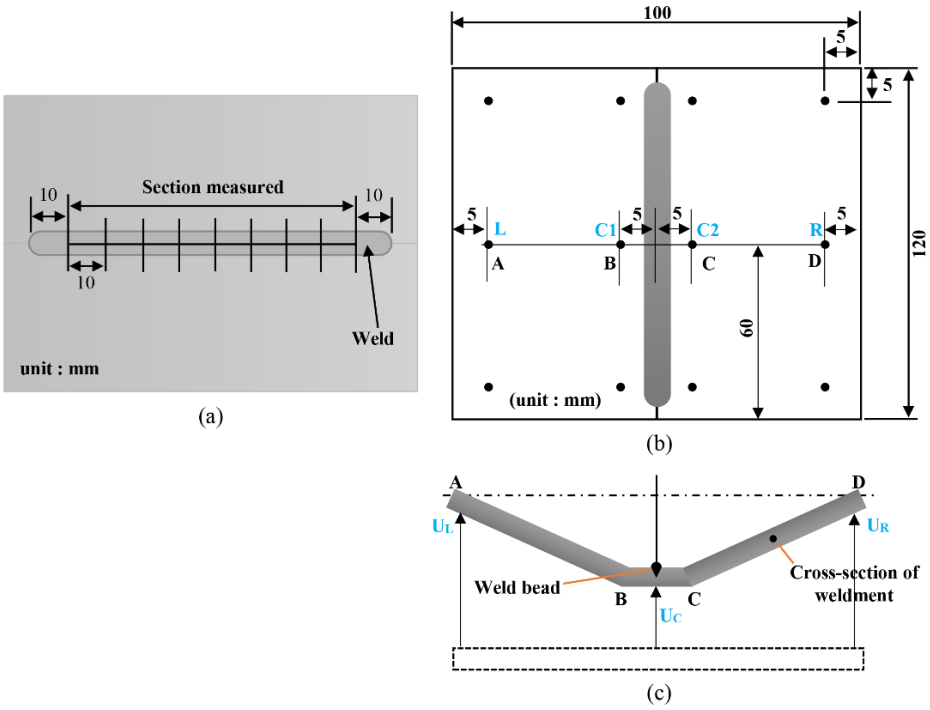

Figure 3. Schematic illustration of (a) weld bead width, (b) measurement distortion and (c) mean vertical displacement method [22].

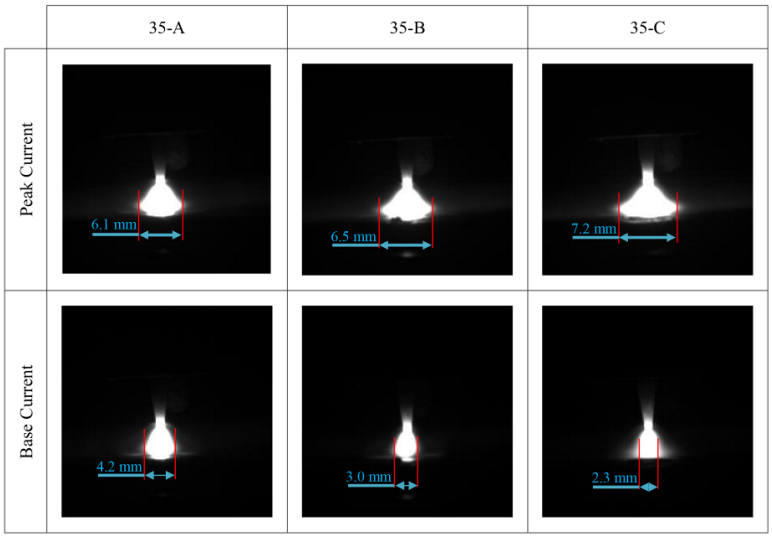

Figure 4. Arc profile on pulsed GTAW.

Visualisation Test on Top Weld Bead and Back Weld Bead

The surface profile of the top weld bead and back weld bead shown in Figure 5 and Figure 6, respectively. There were 3 conditions of duty cycle with 3 different pulsed current and continuous current parameters. In parameter A through C, peak current was increased but the base current was decreased so that mean current remains the same. Visually the top weld bead and back weld bead produced were almost uniform.

Figure 7(a) and Figure 7(b) show the average of top bead width and back bead width on pulsed GTAW then compared it with continuous GTAW on the same mean current. The result of the top bead width on pulsed GTAW still wider than continuous GTAW. The widest of top bead width at a peak current of 212 A and the base current of 40 A (code 35-C) and the smallest of top bead width at a peak current of 111 A and the base current of 80A (code 65-A). The widest of back bead width at a peak current of 160 A and the base current of 40A (code 50-C) and the smallest of top bead width at a peak current of 111A and the base current of 80A (code 65-A). The result of the top bead width and back bead width on pulsed GTAW were wider than continuous GTAW. The top bead width increases by 4.37%-25.09%, while the back bead width increases by 0.57%-10.42% when using pulsed GTAW.

Increasing the peak current indirectly will affect the arc profile. High peak current produced a wide arc profile. In this study, the highest peak current of 212A produced the widest weld bead. So increasing the peak current can be affected on weld bead width though with the same mean current [6].

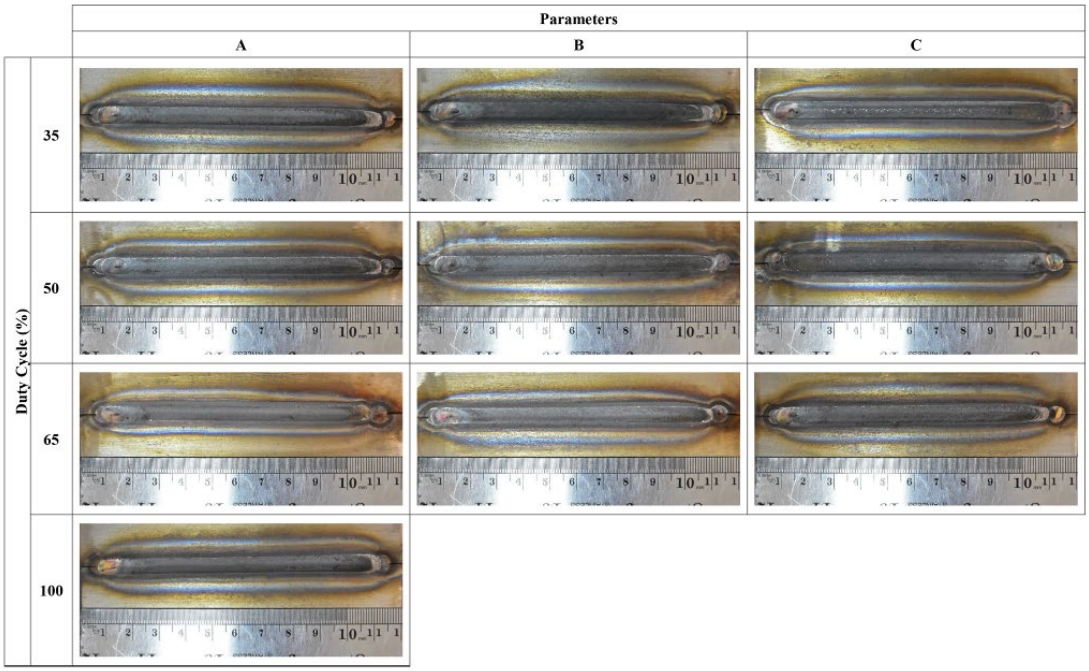

Figure 5. Top weld bead surface profile.

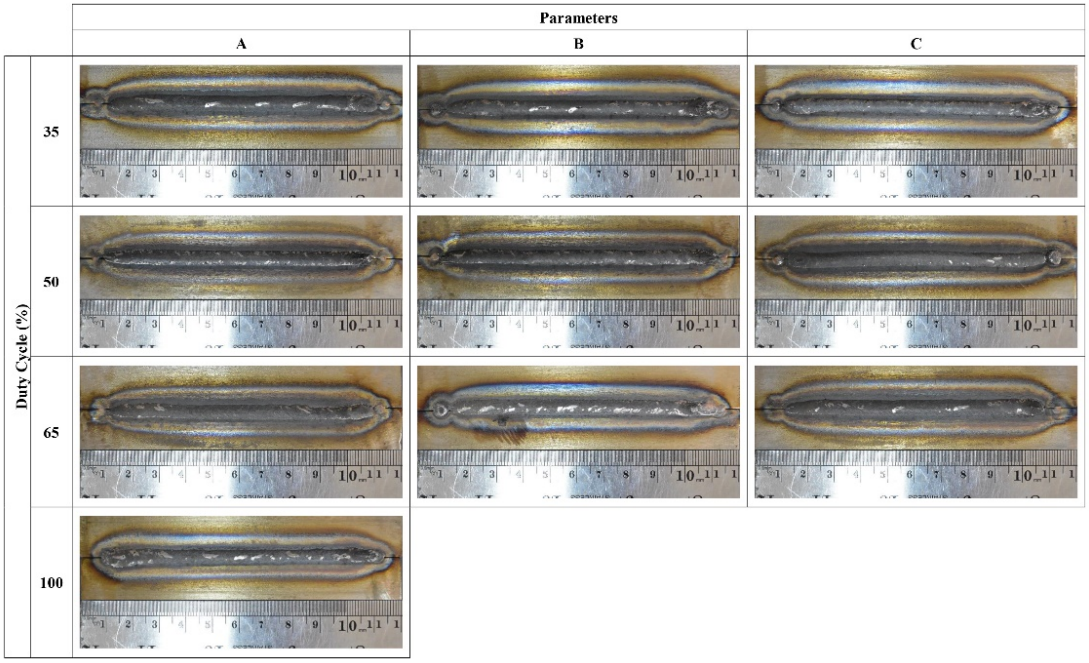

Figure 6. Back weld bead surface profile.

Distortion

The calculation result of longitudinal bending distortion in millimetre (Eq. (3)) and angular distortion in radian (Eq. (4)) as shown in Figure 8(a) and 8(b), respectively. There were 3 conditions of duty cycle with 3 different pulsed GTAW parameters and 1 parameter of continuous GTAW. The biggest of longitudinal bending distortion and angular distortion at a peak current of 133A and the base current of 40 A (code 65-C) and the smallest of longitudinal bending distortion and angular distortion at a peak current of 138 A and the base current of 80A (code 35-A). Based on the results show that pulsed GTAW can produce longitudinal bending distortion and angular distortion smaller than continuous GTAW. Pulsed GTAW can reduce longitudinal bending distortion and angular distortion by 15.15%-72.41% and 29.55%-88.17%, respectively.

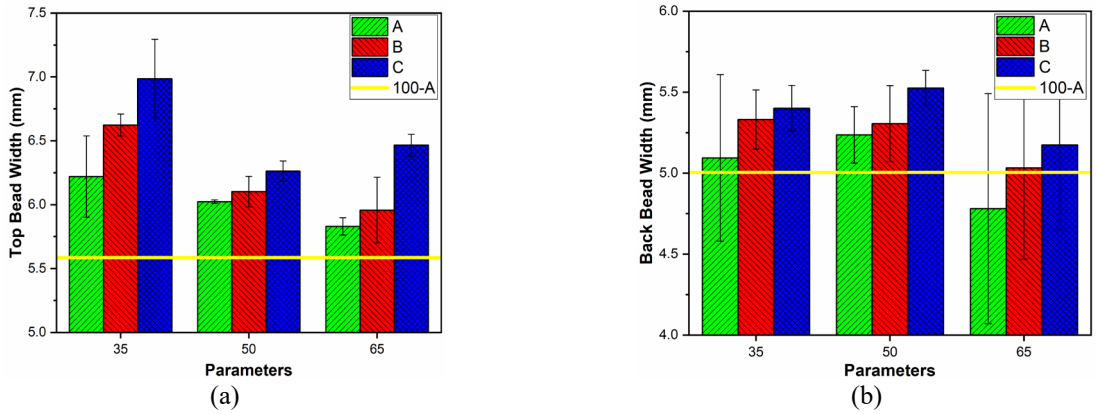

(a) (b)

Figure 7. Comparison of PGTAW and CGTAW on (a) top bead width and (b) back bead width.

An increase in peak current can have an impact on longitudinal bending distortion and angular distortion [6]. Peak current and peak current time have a significant role in temperature. Base current and base current time assist in the cooling process or stabilizing the temperature distribution. When the peak current was working, the specimen will receive a high temperature, while when the base current was working the specimen will receive a low temperature. So that the distortion occurs due to non-linear temperature gradients, thermal expansion and heat input were unequal [8, 25]. In continuous current welding the temperature tends to be linear and the temperature gradient that occurs is linear. So the distortion that occurs is greater than using pulse currents welding. In this study the highest distortion occurs due to the long peak current time while the short peak current time will produce the smallest distortion.

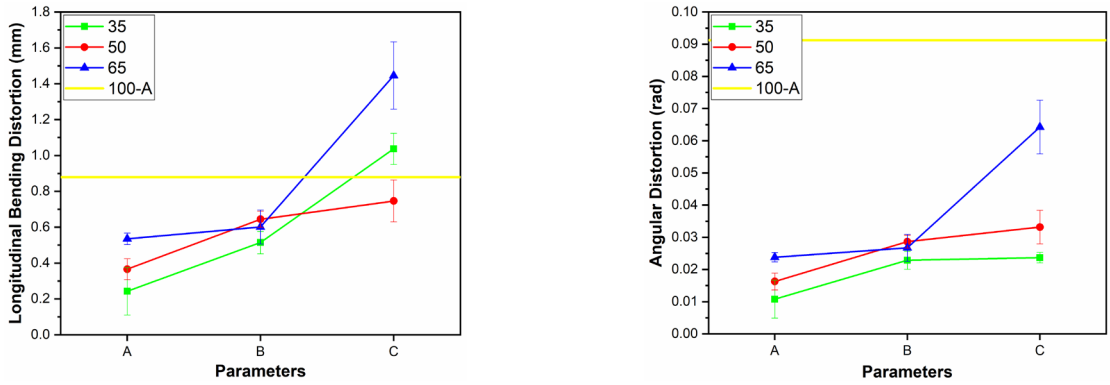

(a) (b)

Figure 8. Comparison of PGTAW and CGTAW on (a) longitudinal bending distortion and (b) angular distortion.

CONCLUSION

In this research, the influence of pulse currents on weld geometry and angular distortion of SS-304 autogenous butt weld joint were discussed. The conclusions were as follows:

i. Between pulsed GTAW and continuous GTAW has differences in weld bead width and distortion. While increasing the peak current can widen the weld bead whereas decreasing the peak current time and peak current can decrease distortion.

ii. Arc profile depends on the amount of peak current and base current. The width of the arc profile directly has an influence on the width of the weld bead.

iii. Pulsed GTAW can widen the top bead width and back bead width by 4.37%-25.09% and 0.57%-10.42%, respectively. The weld bead is widest at a peak current of 212A and the base current of 40A (code 35-C).

iv. The longitudinal bending distortion and the angular distortion show a decrease of 15.15%-72.41% and 29.55%-88.17%, respectively if using pulsed GTAW. The smallest distortion at peak currents 138A and base currents 80A (code 35-A) with the lowest duty cycle.

ACKNOWLEDGEMENT

This research is supported by Master Program to Doctorate for Scholar Excellent (PMDSU) program of the Ministry of Research & Technology and High Education (RISTEK DIKTI) 2019 with contract number NKB-1855/UN2.R3.1/HKP.05.00/2019.

REFERENCES

[1] Eisazadeh H, Haines DJ, Torabizadeh M. Effects of gravity on mechanical properties of GTA welded joints. Journal of Materials Processing Technology 2014; 214(5): 1136-1142.

[2] Singh T, Dureja J, Dogra M, Bhatti MSJIJoA, Engineering M. Machining Performance Investigation of AISI 304 Austenitic Stainless Steel under Different Turning Environments. 2018; 15(4): 5837-5862.

[3] Kumar R, Anant R, Ghosh P, Kumar A, Agrawal B. Influence of PC-GTAW parameters on the microstructural and mechanical properties of thin AISI 1008 steel joints. Journal of Materials Engineering and Performance 2016; 25(9): 3756-3765.

[4] Dorn L, Devakumaran K, Hofmann F. Pulsed current gas metal arc welding under different shielding and pulse parameters; Part 1: Arc characteristics. ISIJ international 2009; 49(2): 251-260.

[5] Reddy GM, Gokhale A, Rao KP. Optimisation of pulse frequency in pulsed current gas tungsten arc welding of aluminium–lithium alloy sheets. Materials Science and Technology 1998; 14(1): 61-66.

[6] Madadi F, Ashrafizadeh F, Shamanian M. Optimization of pulsed TIG cladding process of stellite alloy on carbon steel using RSM. Journal of Alloys and Compounds 2012; 510(1): 71-77.

[7] Giridharan P, Murugan N. Optimization of pulsed GTA welding process parameters for the welding of AISI 304L stainless steel sheets. The International Journal of Advanced Manufacturing Technology 2009; 40(5-6): 478-489.

[8] Kumar TS, Balasubramanian V, Sanavullah M. Influences of pulsed current tungsten inert gas welding parameters on the tensile properties of AA 6061 aluminium alloy. Materials & design 2007; 28(7): 2080-2092.

[9] Minnick WH, Prosser MA, Gas tungsten arc welding handbook. 1996: Goodheart-Willcox Company Tinley Park, Illinois, United States.

[10] Tarng Y, Yang W. Optimisation of the weld bead geometry in gas tungsten arc welding by the Taguchi method. The International Journal of advanced manufacturing technology 1998; 14(8): 549-554.

[11] Aesh MA. Optimization of weld bead dimensions in GTAW of aluminum–magnesium alloy. Materials and Manufacturing Processes 2001; 16(5): 725-736.

[12] Murugan N, Parmar R. Effects of MIG process parameters on the geometry of the bead in the automatic surfacing of stainless steel. Journal of Materials Processing Technology 1994; 41(4): 381-398p.

[13] Gunaraj V, Murugan N. Prediction and optimization of weld bead volume for the submerged arc process—part 1. Welding journal 2000; 79(10): 286s-294s.

[14] Balasubramanian M, Jayabalan V, Balasubramanian V. Process optimisation of PCTIG welding of titanium alloy using the modified Taguchi method. International Journal of Manufacturing Research 2007; 2(4): 403-413.

[15] Pal K, Pal SK. Effect of pulse parameters on weld quality in pulsed gas metal arc welding: a review. Journal of materials engineering and performance 2011; 20(6): 918-931.

[16] Hu S, Han R, Shen J, Han J, Xu H. Effect of pulse frequency on microstructure of 21% Cr ferritic stainless steel in pulsed gas tungsten arc welding. Transactions of Tianjin University 2013; 19(2): 127-129.

[17] Schenk T, Richardson I, Kraska M, Ohnimus SJS, Welding To, Joining. Influence of clamping on distortion of welded S355 T-joints. 2009; 14(4): 369-375.

[18] Li J, Guan Q, Shi Y, Guo DJS, welding to, joining. Stress and distortion mitigation technique for welding titanium alloy thin sheet. 2004; 9(5): 451-458.

[19] Tsai CL, Han MSJJotCIoE. Thermal and mechanical evolution of welding-induced buckling distortion. 2004; 27(6): 907-920.

[20] Baskoro AS. Monitoring of molten pool image during pipe welding in gas metal arc welding (GMAW) using machine vision. in Advanced Computer Science and Information System (ICACSIS), 2011 International Conference on. 2011. IEEE.

[21] Baskoro AS, Tandian R, Edyanto A, Saragih AS. Automatic Tungsten Inert Gas (TIG) welding using machine vision and neural network on material SS304. in Advanced Computer Science and Information Systems (ICACSIS), 2016 International Conference on. 2016. IEEE.

[22] Tseng K, Chou C. Effect of pulsed gas tungsten arc welding on angular distortion in austenitic stainless steel weldments. science and Technology of welding and joining 2001; 6(3): 149-153.

[23] Okano S, Mochizuki M. Transient distortion behavior during TIG welding of thin steel plate. Journal of Materials Processing Technology 2017; 241: 103-111.

[24] Qi B, Yang M, Cong B, Liu F. The effect of arc behavior on weld geometry by high-frequency pulse GTAW process with 0Cr18Ni9Ti stainless steel. The International Journal of Advanced Manufacturing Technology 2013; 66(9-12): 1545-1553.

[25] Kalyankar V, Shah PJMTP. A review on methodologies to reduce welding distortion. 2018; 5(11): 24741-24749.